
An Examination of the CRASH3 Effective Mass Concept

Nathan A. Rose, Stephen J. Fenton and Richard M. Ziernicki
Knott Laboratory, Inc.

Reprinted From: **Accident Reconstruction 2004**
(SP-1873)

ISBN 0 7680 1427-1



9 780768 014273

SAE *International*[™]

2004 SAE World Congress
Detroit, Michigan
March 8-11, 2004

All rights reserved. No part of this publication may be reproduced, stored in a retrieval system, or transmitted, in any form or by any means, electronic, mechanical, photocopying, recording, or otherwise, without the prior written permission of SAE.

For permission and licensing requests contact:

SAE Permissions
400 Commonwealth Drive
Warrendale, PA 15096-0001-USA
Email: permissions@sae.org
Fax: 724-772-4891
Tel: 724-772-4028



For multiple print copies contact:

SAE Customer Service
Tel: 877-606-7323 (inside USA and Canada)
Tel: 724-776-4970 (outside USA)
Fax: 724-776-1615
Email: CustomerService@sae.org

ISBN 0-7680-1319-4
Copyright © 2004 SAE International

Positions and opinions advanced in this paper are those of the author(s) and not necessarily those of SAE. The author is solely responsible for the content of the paper. A process is available by which discussions will be printed with the paper if it is published in SAE Transactions.

Persons wishing to submit papers to be considered for presentation or publication by SAE should send the manuscript or a 300 word abstract of a proposed manuscript to: Secretary, Engineering Meetings Board, SAE.

Printed in USA

An Examination of the CRASH3 Effective Mass Concept

Nathan A. Rose, Stephen J. Fenton and Richard M. Ziernicki
Knott Laboratory, Inc.

Copyright © 2004 SAE International

ABSTRACT

This paper examines the validity of the effective mass concept used in the CRASH 3 damage analysis equations. In this study, the effective mass concept is described, the simplifying assumptions that it entails are detailed, and the accuracy of the concept is tested by comparing ΔV s calculated from the CRASH 3 equations to results of numerical simulations with a non-central impact model. This non-central impact model allowed the effective mass concept to be tested in isolation from other assumptions of the CRASH 3 program. The results of this research have shown that the effective mass concept accurately models the effects of collision force offset when certain conditions are met. These conditions are discussed, along with their implications for damage interpretation.

This paper also presents an analytic expression that relates damage energy to closing speed (initial relative velocity) for the general case of non-central collisions. Equations relating damage energy to closing speed for the case of central collisions have been discussed extensively in the literature. However, a comparable equation for the general case of vehicle-to-vehicle non-central impacts has not been reported. The effective mass concept is used to generalize the relationship between closing speed and damage energy.

INTRODUCTION

Using the mass-spring system shown in Figure 1, McHenry derived simple, closed-form equations that relate the energy expended in crushing a vehicle to the change in velocity experienced by the vehicle during the impact (ΔV) [5,6,7,8,9]. These equations, given by Equations (1) and (2) below, form the basis of the CRASH 3 damage analysis algorithm and are valid for the case of central collisions, where the collision forces are directed through the centers of gravity of the vehicles.

In Figure 1 and in Equations (1) and (2), M_1 and M_2 are the vehicle masses, K_1 and K_2 are the structural stiffnesses of the engaged vehicle structures, and E_1 and E_2 are the energies associated with crushing the vehicle structures.

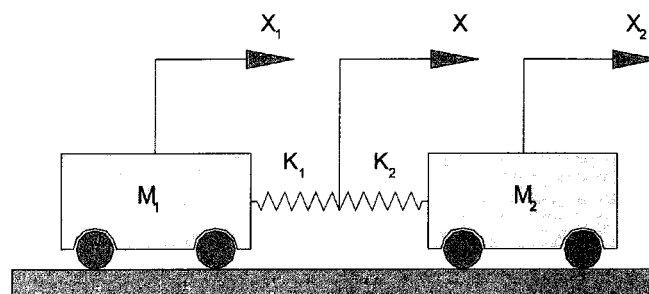


Figure 1
The CRASH 3 Impact Model

$$\Delta V_1 = \frac{\sqrt{2(E_1 + E_2)}}{\sqrt{M_1 \left(1 + \frac{M_1}{M_2}\right)}} \quad (1)$$

$$\Delta V_2 = \frac{\sqrt{2(E_1 + E_2)}}{\sqrt{M_2 \left(1 + \frac{M_2}{M_1}\right)}} \quad (2)$$

McHenry extended Equations (1) and (2) to the general case of non-central collisions using the concept of an effective vehicle mass. The effective mass concept was based on the idea that when the collision force does not pass through the center of gravity of a vehicle, the full weight of the vehicle does not participate in the collision. Application of the effective mass concept resulted in only slight modifications to the simple analytic equations derived for the central case.

McHenry began the development of the effective mass concept by considering the collision model shown in Figure 2. In this figure, I_1 and I_2 are the yaw moments of inertia of the vehicles, ψ_1 and ψ_2 are the angular orientations of the vehicles, h_1 and h_2 are the distances that the collision forces are offset from the centers of gravity of the vehicles – measured perpendicular to the line of action of the collision forces – and $\Delta V_1'$ and $\Delta V_2'$ are the changes in velocity experienced by each vehicle

at point P, the point of application of the resultant collision forces. The x_1 - y_1 and x_2 - y_2 frames are body-fixed reference frames. It is assumed that during the depicted collision, a common velocity is reached at the common point P, but not necessarily by the vehicle centers of gravity.

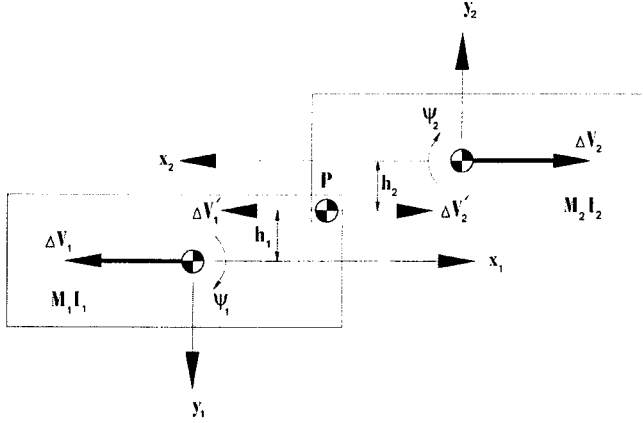


Figure 2

McHenry's Eccentric Collision Configuration

With this impact model, McHenry arrived at the following generalized equations:

$$\Delta V_1 = \frac{2\gamma_1(E_1 + E_2)}{M_1 \left(1 + \frac{\gamma_1 M_1}{\gamma_2 M_2} \right)} \quad (3)$$

$$\Delta V_2 = \frac{2\gamma_2(E_1 + E_2)}{M_2 \left(1 + \frac{\gamma_2 M_2}{\gamma_1 M_1} \right)} \quad (4)$$

In Equations (3) and (4), the multipliers, γ_1 and γ_2 , are the effective mass multipliers and are given as follows:

$$\gamma_i = \frac{k_i^2}{k_i^2 + h_i^2} \quad (5)$$

In Equation (5), k_i is the radius of gyration of Vehicle 1 or 2. The validity of Equations (3) and (4), and the effective mass concept that forms their base, was the fundamental question of this study.

The effective mass concept represents an approximate method for incorporating collision forces that are offset from the vehicle center of gravity, since McHenry's derivation of Equations (3) and (4) relied on writing the acceleration of point P on Vehicle 1 as follows:

$$\ddot{X}_P = \ddot{X}_1 + h_1 \ddot{\psi}_1 \quad (6)$$

In Equation (6), \ddot{X}_P is the acceleration at the point P,

\ddot{X}_1 is the acceleration at the center of gravity of Vehicle 1, and $\ddot{\psi}_1$ is the angular acceleration of Vehicle 1.

Strictly speaking, Equation (6) is incomplete. A complete expression for the acceleration of a point on a rigid body relative to the center of gravity of that body takes the following form [1,2]:

$$\bar{a}_P = \bar{a}_G + \ddot{\psi}_1 \times \bar{r}_{P/G} + \dot{\psi}_1 \times (\dot{\psi}_1 \times \bar{r}_{P/G}) \quad (7)$$

In Equation (7), \bar{a}_P is the acceleration of the point P, \bar{a}_G is the acceleration of the center of gravity, $\bar{r}_{P/G}$ is a position vector that locates the point P in a reference frame attached to the body at the center of gravity, $\dot{\psi}_1$ is the angular velocity of the body about the center of gravity, and again, $\ddot{\psi}_1$ is the angular acceleration of the body about the center of gravity. The first term on the right side of Equation (7) accounts for the translational acceleration of the center of gravity relative to the inertial (fixed) frame. The second term accounts for the angular acceleration of the reference frame attached to the body. And finally, the third term accounts for the centripetal acceleration of point P. A comparison of Equations (6) and (7) reveals that Equation (6) contains no term to account for the centripetal acceleration of the point P.

Equation (7) results from taking the derivative with respect to time of the velocity expression for a point on a rigid body relative to the body center of gravity, Equation (8) below.

$$\bar{v}_P = \bar{v}_G + \dot{\psi}_1 \times \bar{r}_{P/G} \quad (8)$$

The centripetal acceleration term in Equation (7) arises during application of the chain rule during differentiation of the second term in Equation (8) and, ultimately, arises as a result of differentiating the position vector with respect to time. This is shown below in Equations (9) through (12), which show the differentiation with respect to time of Equation (8) in a series of steps. Equation (12) is equivalent to Equation (7).

$$\frac{d\bar{v}_P}{dt} = \frac{d\bar{v}_G}{dt} + \frac{d}{dt} (\dot{\psi}_1 \times \bar{r}_{P/G}) \quad (9)$$

$$\bar{a}_P = \bar{a}_G + \frac{d\dot{\psi}_1}{dt} \times \bar{r}_{P/G} + \dot{\psi}_1 \times \frac{d\bar{r}_{P/G}}{dt} \quad (10)$$

$$\bar{a}_P = \bar{a}_G + \ddot{\psi}_1 \times \bar{r}_{P/G} + \dot{\psi}_1 \times \bar{v}_{P/G} \quad (11)$$

$$\bar{a}_P = \bar{a}_G + \ddot{\psi}_1 \times \bar{r}_{P/G} + \dot{\psi}_1 \times (\dot{\psi}_1 \times \bar{r}_{P/G}) \quad (12)$$

In McHenry's derivation, h_1 and h_2 are equivalent to $\vec{r}_{P/G}$, since h_1 and h_2 are taken perpendicular to the collision force. McHenry treated h_1 and h_2 as constants. Treating the collision force moment arms as constants is an approximation, since for the system shown in Figure 2, and for actual impacts, the moment arms of the collision force will vary through time, due to variation in the direction of the instantaneous collision force and movement of the point of application of the instantaneous, resultant collision force. The significance of this for McHenry's derivation is that since he assumed the collision force moment arm does not vary with time, the centripetal acceleration term does not arise when Equation (31) is differentiated with respect to time, since the time derivative of $\vec{r}_{P/G}$ is equal to zero.

So, the fundamental assumption of the derivation of the effective mass concept is that a representative, effective, or resultant collision force moment arm can replace the time-varying collision force moment arm that is present during the actual impact. This is the assumption tested by the research reported in this paper. Various definitions of this resultant moment arm are plausible and the derivation does not specify which definition should be used. These various definitions will be explored later and the results obtained using each one will be compared.

It should be noted that McHenry's derivation of the effective mass concept is quasi-one-dimensional, meaning that, while rotational effects have been incorporated into the derivation, the change in velocity is still assumed to occur along the X-direction. This is clear from the fact the derivation involves only scalar quantities and is written in terms of X and its derivatives – Y and its derivatives do not appear. For an actual offset impact, the change in velocity will occur in more than one coordinate direction. In practice, this simply means that the one-dimensional ΔV obtained from the CRASH 3 equations will occur along the direction of the principle collision force, which for CRASH 3 analysis, the user must specify. The direction of the principle force becomes the one dimension along which McHenry's derivation is valid. This will be important later during derivation of a generalized damage energy/ closing speed formula.

VALIDATION OF THE EFFECTIVE MASS CONCEPT

To explore the physical accuracy of the effective mass concept in the CRASH 3 damage equations, the present research examined an offset barrier impact model that incorporated a collision force offset from the vehicle center of gravity. This impact model (Figure 3) consisted of a mass and a spring with the point of connection between the mass and the spring offset from the center of gravity of the mass. Also, the point of connection between the mass and the spring is enclosed in a frictionless track. The motivation for the addition of the frictionless track is the empirical observation that in an actual offset barrier collision, the vehicle center of

rotation would roughly coincide with the point where the resultant collision force is transferred, the point 1P in the barrier impact model. The track in the model forces the center of rotation to reside at the point 1P.

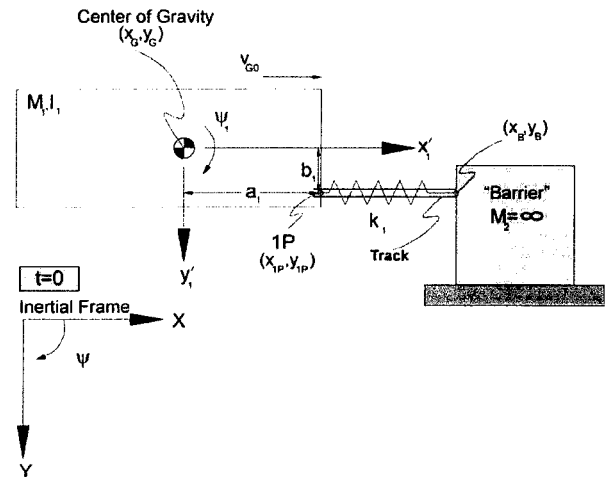


Figure 3
Offset Barrier Impact Model

Adding this track affects the system physically in two ways. First, the spring force is confined to the X-direction. Second, a Y-direction reaction force arises as a result of the interaction between the body and the track. This reaction force will cause the resultant external force (collision force) to have a component in the negative Y-direction.

The impact model of Figure 3 consists of a rectangular body of mass M_1 , with yaw moment of inertia I_1 , a linear spring, with stiffness coefficient k_1 , and a rigid barrier of infinite mass. The center of gravity of the body is located in the inertial reference frame with the coordinates x_G and y_G and the orientation of the body is described by the angle ψ_1 measured clockwise off of the inertial x -axis. The reference frame $x'_1 - y'_1$ is attached to the body and the point 1P is fixed in this reference frame at the coordinates a_1 and b_1 . The spring is connected to the point 1P on the body (x_{1P} and y_{1P} in the inertial reference frame) and point B (x_B and y_B in the inertial reference frame) on the barrier.

The following assumptions are invoked for the system shown in Figure 3:

1. The point 1P is confined to move in the x -direction by the frictionless track.
2. The only forces acting on the mass are the spring force, generated by relative movement between point 1P on the body and point B on the barrier, and the constraint (reaction) force holding the point 1P in the track. Together, these constitute the "collision" force.

3. The initial translational velocity and the initial orientation of the body are in the positive x-direction.
4. The body has no initial rotational velocity.
5. At time $t = 0$, the spring applies no force to the body.

The barrier impact model shown in Figure 3 is a two degree-of-freedom system. A Newton-Euler formulation of the equations of motion for this system consists of the three Newton-Euler equations – one for each coordinate direction and one for rotation – augmented by a single algebraic constraint equation. The approach taken in this research for solving the equations of motion was to write the Newton-Euler equations, along with the constraint equation, and then to eliminate the unknown constraint force and redundant coordinate from the equations of motion by differentiating the constraint equation twice with respect to time and substituting it into the equations of motion. This has the effect of reducing the equations of motion to two second-order differential equations, and therefore, of simplifying the numerical solution. After the solution of these two equations, the redundant coordinate and reaction force were obtained by back-substitution.

A free body diagram for the mass in the offset barrier impact model follows in Figure 4.

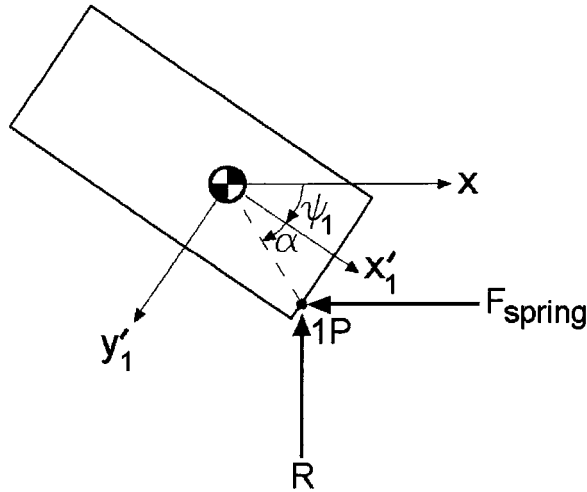


Figure 4
Free-Body Diagram

In Figure 4, F_{SPRING} is the spring force and R is the reaction force that maintains the point 1P in the track. The magnitude of the spring force is equal to the spring stiffness k_1 multiplied by the compression of the spring beyond its equilibrium position and is given by Equation (13).

$$F_{SPRING} = k_1(x_{1P0} - x_{1P}) \quad (13)$$

In Equation (13), x_{1P0} is the initial x-direction position of the point 1P and x_{1P} is the x-direction position of the point 1P at any time, t . In terms of the coordinates of the center of gravity,

$$x_{1P0} = x_{G0} + a_1 \quad (14)$$

$$x_{1P} = x_G + a_1 \cos \psi_1 - b_1 \sin \psi_1 \quad (15)$$

In Equation (14), x_{G0} is the initial x-direction position of the mass center of gravity. The moments, M_G , about the center of gravity are given by Equation (16).

$$M_G = -F_{SPRING}(b_1 \cos \psi_1 + a_1 \sin \psi_1) + R(a_1 \cos \psi_1 - b_1 \sin \psi_1) \quad (16)$$

Now, the Newton-Euler Equations of motion for the offset barrier impact model can be written as follows:

$$m\ddot{x}_G = F_{SPRING} \quad (17)$$

$$m\ddot{y}_G = R \quad (18)$$

$$I_G\ddot{\psi}_1 = M_G \quad (19)$$

In Equations (17) through (19), \ddot{x}_G is the x-direction acceleration of the mass center of gravity, \ddot{y}_G is the y-direction acceleration of the mass center of gravity, and $\ddot{\psi}_1$ is the angular acceleration of the mass about the center of gravity.

To confine the point 1P to move within the track, the Newton-Euler equations of motion must be supplemented with a single constraint equation. Letting the origin of the inertial reference frame coincide with the Point B, this constraint equation can be written as follows, in terms of the center of gravity coordinates:

$$y_G + b_1 \cos \psi_1 + a_1 \sin \psi_1 = 0 \quad (20)$$

Differentiating Equation (20) twice with respect to time yields Equation (21).

$$\begin{aligned} \ddot{y}_G &= b_1\ddot{\psi}_1 \sin \psi_1 + b_1\dot{\psi}_1^2 \cos \psi_1 \\ &- a_1\ddot{\psi}_1 \cos \psi_1 + a_1\dot{\psi}_1^2 \sin \psi_1 \end{aligned} \quad (21)$$

In Equation (21), $\dot{\psi}_1$ is the angular velocity of the mass about the center of gravity. Equation (21) can be substituted into Equation (18) and the resulting equation substituted into Equation (19) to yield two second-order differential Equations for x_G and ψ_1 , which can be solved using traditional numerical methods for

differential equations. The y-coordinate of the center of gravity and the reaction force from interaction with the track can then be backed out after the x-direction and the rotational coordinates have been calculated at each time step.

NUMERICAL SIMULATIONS

Test Program

Simulations were run with the barrier impact model of Figure 3 for the following five vehicle configurations:

Vehicle #1 (Miniature)

Vehicle Weight:	2469 lbs
Yaw Moment of Inertia:	1297.15 lb-ft-sec ²
Vehicle Length:	13.32 ft
Vehicle Width:	5.07 ft
Front to CG:	6.33 ft
Stiffness per Unit Width:	72.11 lb/in ²
Damage Width:	36 inches
a ₁ :	3.31 feet

Vehicle #2 (Sub-Compact)

Vehicle Weight:	2753 lbs
Yaw Moment of Inertia:	1736.95 lb-ft-sec ²
Vehicle Length:	14.58 ft
Vehicle Width:	5.60 ft
Front to CG:	6.94 ft
Stiffness per Unit Width:	66.38 lb/in ²
Damage Width:	36 inches
a ₁ :	3.62 feet

Vehicle #3 (Compact)

Vehicle Weight:	3247 lbs
Yaw Moment of Inertia:	2553.95 lb-ft-sec ²
Vehicle Length:	16.35 ft
Vehicle Width:	6.05 ft
Front to CG:	7.48 ft
Stiffness per Unit Width:	69.97 lb/in ²
Damage Width:	36 inches
a ₁ :	3.97 feet

Vehicle #4 (Intermediate)

Vehicle Weight:	3947 lbs
Yaw Moment of Inertia:	3632.84 lb-ft-sec ²
Vehicle Length:	17.73 ft
Vehicle Width:	6.42 ft
Front to CG:	8.23 ft
Stiffness per Unit Width:	66.7 lb/in ²
Damage Width:	36 inches
a ₁ :	4.26 feet

Vehicle #5 (Full-Size)

Vehicle Weight:	4565 lbs
Yaw Moment of Inertia:	4628.02 lb-ft-sec ²
Vehicle Length:	18.64 ft
Vehicle Width:	6.65 ft
Front to CG:	8.42 ft
Stiffness per Unit Width:	113 lb/in ²
Damage Width:	36 inches
a ₁ :	5.11 feet

The parameters for these vehicles roughly correspond to parameters for the classes from the CRASH 3 default parameters. These were used because they provide readily available and realistic representative dimensions for the simulations. The stiffness parameters are from the updated values in Reference 10. The yaw moments of inertia are calculated using the prism method.

A total of 24 simulations runs were made, distributed between the five vehicle setups. Twenty-two of the 24 runs were made with initial vehicle velocities of 60ft/s. The remaining two were run with initial velocities of 10ft/s. Numerical analysis was carried out using a fourth-order Runge-Kutta technique with time steps varying between 50 and 500 microseconds.

Simulation Results

The maximum deformation energy for each simulation run is a part of the calculation of ΔV using the CRASH 3 algorithm and so the maximum deformation energy for each simulation is summarized in Table 1 below.

Test Number	Initial Velocity (ft/s)	b ₁ (ft)	Maximum Deformation Energy (ft-lb) ¹
1	10.0	0.0	3833.85
2	10.0	2.5	3403.33
3	60.0	0.0	138018.6
4	60.0	1.0	133117.7
5	60.0	2.0	118376.1
6	60.0	2.5	109972.6

Table 1a – Maximum Deformation Energies (Mini)

Test Number	Initial Velocity (ft/s)	b ₁ (ft)	Maximum Deformation Energy (ft-lb)
7	60.0	0.0	153894.4
8	60.0	1.0	149,241.9
9	60.0	2.0	134556.7
10	60.0	2.5	127605.1

Table 1b – Maximum Deformation Energies (Subcompact)

Test Number	Initial Velocity (ft/s)	b ₁ (ft)	Maximum Deformation Energy (ft-lb)
11	60.0	0.0	181509.3
12	60.0	1.0	176921.2
13	60.0	2.0	210284.2
14	60.0	3.0	144987.9

Table 1c – Maximum Deformation Energies (Compact)

¹ Maximum deformation energies in Tables 1a through 1e are approximate, but are within 1-2% of their actual values. The authors neglected to output these values in the simulation output file and to avoid having to rerun the simulations these values were calculated from other simulation output. Calculated values reported later in this paper did not rely on these approximate values, but rather on the actual simulation values.

Test Number	Initial Velocity (ft/s)	b ₁ (ft)	Maximum Deformation Energy (ft-lb)
15	60.0	0.0	220639.8
16	60.0	1.0	214830.3
17	60.0	2.0	201512.4
18	60.0	3.0	180951.8
19	60.0	4.0	159974.8
20	60.0	5.0	139830.4

Table 1d – Maximum Deformation Energies (Intermediate)

Test Number	Initial Velocity (ft/s)	b ₁ (ft)	Maximum Deformation Energy (ft-lb)
21	60.0	0.0	255186.3
22	60.0	1.0	250431.3
23	60.0	2.0	237351.0
24	60.0	3.0	219090.4

Table 1e – Maximum Deformation Energies (Full Size)

In order to address the accuracy of the CRASH 3 effective mass concept, two additional values were extracted from the simulation runs. First, the resultant change in velocity experienced by the body center of gravity from time zero to the time of maximum deformation was obtained. This is the value that was compared to the CRASH 3 calculated velocity changes. Second, appropriate values for the resultant collision force moment arm were calculated, since this value is needed to calculate the effective mass factors, γ , which are also used in the calculation of the velocity change with the CRASH 3 algorithm equations.

The first of these, the resultant ΔV experienced by the vehicle in each simulation run, is easily obtained from the simulation data. The results are summarized in Tables 2a through 2e below.

Test Number	Initial Velocity (ft/s)	b ₁ (ft)	$\Delta V_{\text{resultant}}$ (ft/s)
1	10.0	0.0	9.97 ²
2	10.0	2.5	9.20
3	60.0	0.0	59.84
4	60.0	1.0	57.66
5	60.0	2.0	52.06
6	60.0	2.5	48.69

Table 2a – Actual Velocity Changes (Mini)

Test Number	Initial Velocity (ft/s)	b ₁ (ft)	$\Delta V_{\text{resultant}}$ (ft/s)
7	60.0	0.0	59.37
8	60.0	1.0	58.05
9	60.0	2.0	53.27
10	60.0	2.5	50.18

Table 2b – Actual Velocity Changes (Subcompact)

² There is some numerical error in the calculated actual ΔV s. For the central impact case, $b_1=0$, the actual ΔV should be equal to the impact speed. Thus, part of the error in the ΔV calculations reported later is due to error in the calculation of the actual ΔV . This will be discussed later in this paper.

Test Number	Initial Velocity (ft/s)	b ₁ (ft)	$\Delta V_{\text{resultant}}$ (ft/s)
11	60.0	0.0	59.66
12	60.0	1.0	58.40
13	60.0	2.0	54.36
14	60.0	3.0	49.00

Table 2c – Actual Velocity Changes (Compact)

Test Number	Initial Velocity (ft/s)	b ₁ (ft)	$\Delta V_{\text{resultant}}$ (ft/s)
15	60.0	0.0	59.58
16	60.0	1.0	58.56
17	60.0	2.0	55.06
18	60.0	3.0	50.19
19	60.0	4.0	44.87
20	60.0	5.0	39.80

Table 2d – Actual Velocity Changes (Intermediate)

Test Number	Initial Velocity (ft/s)	b ₁ (ft)	$\Delta V_{\text{resultant}}$ (ft/s)
21	60.0	0.0	59.28
22	60.0	1.0	58.85
23	60.0	2.0	56.16
24	60.0	3.0	52.24

Table 2e – Actual Velocity Changes (Full Size)

The second, obtaining a representative value for the collision force moment arm is not as straight forward, since it is not immediately clear what value of the moment arm is the most representative. A number of possibilities exist for defining this "average" moment arm, including the following:

1. The first possibility is to let the average moment arm, h_{avg} , equal the initial offset of the collision force (b_1). This would be expected to be the least accurate, since the initial offset is the least representative of the moment arm throughout the collision. This moment arm occurs at the beginning of the impact, when the collision force is low.
2. The second possibility is to let h_{avg} equal the arithmetic mean value of the instantaneous moment arms (the moment arm at each time step) between time zero and maximum spring compression. This average moment arm is given by

$$h_{\text{avg}} = \frac{\sum_{i=1}^N h_i}{N}, \quad (22)$$

where N is the number of time steps between time zero and the maximum spring compression. We would expect this h_{avg} to be more representative than the first definition, but still not ideal since it gives equal weight to the h value at every time step.